PROCEEDINGS. Twenty-Third Workshop on Geothermal Reservoir Engineering
Stanford University, Stanford. California, January 26-28, 1998
SGP-TR-158

# A MEASUREMENT OF STEAM-WATER RELATIVE PERMEABILITY

Cengiz Satik

Stanford Geothermal Program
Stanford University
Stanford, CA 94305-2220

## ABSTRACT

This paper reports experimental efforts towards measuring accurate steam-water relative permeability functions under steady-state and non-adiabatic conditions. A steady-state experiment was conducted and a set of relative permeability curves for simultaneous flow of steam and water in porous media has been obtained. These relations show that the relative permeabilities for both steam and water phases in porous media vary with saturation in a curvilinear fashion. The saturations in this experiment were measured by using a high resolution X-ray computer tomography (CT) scanner. In addition the pressure gradients were obtained from accurate measurements of liquid-phase pressure over regions with flat saturation profiles. These two aspects constitute a major improvement in the experimental method compared to those used in the past.

## INTRODUCTION

Darcy's equation is an empirical relationship which also describes the flow of a single-phase, incompressible fluid through a horizontal porous medium:

$$Q = \frac{k}{\mu} A \left(\frac{\Delta p}{L}\right) \quad \text{.....} \quad (1)$$

where $Q$, $k$, $\mu$, $A$, $L$, $\Delta p$ are injection rate, absolute permeability, fluid viscosity, cross-sectional area, length and pressure drop over the length $L$, respectively. This equation simply relates fluid injection rate or velocity io pressure drop at sufficiently small flow rates. With the knowledge of pressure gradient, fluid injection velocity and viscosity, one can use this equation to calculate permeability of a porous medium for the case of a single-phase, incompressible fluid flow. In the case of multi-phase flow, however, Darcy's equation must be modified to account for interactions of different phases during flow in complex pore structure. To consider this effect, a new permeability concept, traditionally called as ***effective permeability,*** was introduced:

$$k_i = \frac{Q_i \mu_i L}{A \Delta p_i} \quad ; \; i = \textit{steam, water.} \quad \text{.....} \quad (2)$$

Here $k_i$ is effective permeability to phase $i$, $Q_i$ is injection rate of phase $i$, and $\mu_i$ is viscosity of phase $i$. Furthermore, a non-dimensional form of effective permeability, called as relative permeability ($k_r$), was also described as the ratio of effective permeability to absolute permeability ($k_{ri}=k_i/k$). Relative permeabilities have been expressed in functional form as a function of (wetting or non-wetting phase) saturation (ref.s 3, 4 and 5). These functions are known to depend on many parameters characteristic of both porous material and fluids such as fluid saturation, viscosity, interfacial tension, permeability and temperature etc.

Unsteady- or steady-state methods are traditionally used to determine relative permeability. Both methods measure the relative permeabilities as a function of saturation. Unsteady-state methods are based on the Buckley-Leverett (B-L) theory, therefore, they are restricted by its assumptions. These methods have commonly been used for immiscible, isothermal and non-condensing types of displacement processes. Steady-state methods measure relative permeabilities that are independent of time. During steady-state experiments two fluids are injected simultaneously at a known fraction until steady-state conditions are reached. At steady state, relative permeabilities are calculated by using a theory that relies on Darcy's law extended for multi phase flow. The corresponding saturation values should also be determined. The main assumption of these methods is the requirement for existence of a flat saturation profile, which can be achieved by using a sufficiently long core or high flow rates. Otherwise, the ***capillary end-effects*** commonly observed in many experiments may complicate interpretation of the results.

Steady-state methods have been used to determine steam-water relative permeabilities under adiabatic conditions. Even though such experiments are simpler, previous literature has pointed out major difficulties, particularly in the interpretation of results. Problems have arisen in the determination of accurate saturation profiles and also in the treatment of phase change, heat transfer, capillarity and injection rate.

Reliable measurement of steam-water relative permeability functions is of great importance in geothermal reservoir simulation to match or forecast production performance of geothermal reservoirs. Accordingly, the subject has attracted attention in the past and many experimental and theoretical attempts have been made to study this important problem. A detailed literature survey was given in Ambusso (1996). In spite of large number of reported studies, there still remains considerable uncertainty about the exact form of these functions due to the difficulties encountered in the interpretation of results and the lack of understanding of microscopic pore-level phenomena such as phase change, heat transfer and capillarity.

The literature survey given in Ambusso (1996) shows a wide discrepancy in the previous experimental results, which suggests that the interpretation of the data may not be correct. Additionally, a major problem of obtaining reliable saturation profiles has been emphasized. Recognizing that saturation and temperature profiles are dependent on parameters such as injection rate and temperature, steam quality, system pressure, core permeability and length and also that determining accurate saturation profiles is crucial, we initiated a systematic study to determine steady-state steam-water relative permeabilities directly. With the use of our X-ray computer tomography (CT) scanner equipment we have overcome the difficulty of obtaining accurate saturation distributions along the core samples while multi-phase flow experiments are being conducted. This paper reports the results of a second successful relative permeability experiment conducted recently. Because the results reported in this paper are not confirming our previous results, we plan to repeat this experiment again. In this paper, we first describe the experimental apparatus and method. Then we continue with a discussion of results obtained from the experiment.

## EXPERIMENTAL APPARATUS AND PROCEDURE

The experimental apparatus used in this experiment consisted of an injection unit, and a core holder assembly. The injection unit consisted of two furnaces to generate steam and hot water and two liquid pumps. Two voltage controllers were used to control the temperatures of the furnaces. The core holder assembly differed significantly from the one used in the experiments discussed in Satik et al. (1995) and Ambusso et al. (1996). The core holder was constructed from a plastic (ultem) tube, a high temperature epoxy and several high temperature plastic fittings. In preparing a core holder, the first step was to heat a Berea sandstone core sample in an oven at 800 °C overnight to deactivate clays and to get rid of residual water (Ma and Morrow, 1991). Previously, the oven temperature was set to 400-450 °C (Ambusso, 1996) and serious plugging problems were encountered during the experiments using the core holders made of these cores. The problems of plugging during the flow experiments were solved by simply changing the oven temperature from 400-450 °C to 800 °C. Temperatures along the core were measured by T-type thermocouples inserted at locations where pressure ports are located. There were eight pressure and temperature measurements along the core holder, two at the inlet and one at outlet. Heat losses on the core body were measured by using nine heat flux sensors placed at various locations along the core body. All of the measurements during the experiment were taken by using a data acquisition system. Direct monitoring of pressures and temperatures during the experiment enabled us to determine when steady state conditions had been reached.

The Berea sandstone rock samples used for these experiments had the following properties; permeability 1200 md, porosity 22%, length 43.2cm and diameter 5.04 cm. The core sample was first heated to 800°C for twelve hours to deactivate clays and to get rid of residual water. Then the core sample was epoxied in a plastic (ultem) tube by leaving the two ends of the core sample free of epoxy. Following this, eight pressure ports were drilled at fixed intervals along the edge of the core holder body. The two ends of the core holder were then machined for attachment of the end plates. After mounting all of the necessary pressure fittings, the core holder was tested for leaks. Finally, heat flux sensors were placed along the core holder before it was covered with an insulation material made of ceramic blanket. The core was then placed on a motorized bench that could be

moved to precise locations in the high resolution X-ray CT scanner. A picture of the experimental apparatus within the X-ray CT scanner is shown in Figure 1.

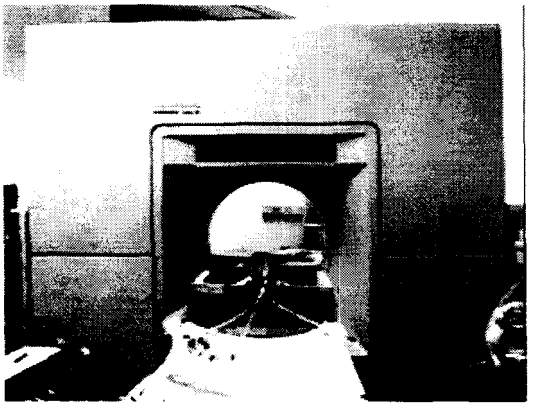

Figure 1: A picture of the X-ray CT scanner and the core holder used in flow experiments

The experimental procedure was as follows. First, air inside the pore space was removed by using a vacuum pump, then the core was scanned at predetermined locations to obtain dry-core CT ($CT_{dry}$) values. Next, deaerated water was injected into the core to saturate it completely. This step continued until the core was completely saturated with water, at which time the core was scanned again at the same locations to obtain wet-core CT ($CT_{wet}$) values and pressure and temperature readings were again taken at this time. Steady-state relative permeability experiments involve injection of varying fractions of steam and water into the core. Measurements done at each step result in a single data point on relative permeability vs. saturation curve. Starting from a completely water saturated core and injecting steam at increasing fractions will give rise to a drainage process while the opposite procedure gives rise to an imbibition process. Each step continued until steady-state conditions at which injection and production rates became the same for both steam and water and also pressures and temperatures stabilized. At the onset of steady-state conditions, another X-ray scan was done along the core at the same locations to obtain CT ($CT_{exp}$) values corresponding to the particular steam-water fraction. Next, the steam-water fraction was changed and the above procedure was repeated.

During the experiment, an interpretation software was used to calculate the porosity and saturation distributions from the *CT* values obtained with the scanner. To calculate porosity the following expression was used:

$$\phi = \frac{CT_{wet} - CT_{dry}}{CT_{water} - CT_{air}} \quad \text{.....} \quad (1)$$

where $CT_{water}$, $CT_{air}$ are CT numbers for water and air, respectively. Similarly, the expression used to calculate saturations is:

$$S_{st} = \frac{CT_{wet} - CT_{exp}}{CT_{wet} - CT_{dry}} \quad (2)$$

and

$$S_w = 1 - S_{st} \quad \text{.....} \quad (3)$$

where $S_{st}$ and $S_w$ denote steam and water saturations, respectively.

## EXPERIMENTAL RESULTS

The single core dynamic method was used for the measurement of the relative permeability. This method required that a two-phase mixture of steam and water be injected into a core. By changing the flowing fractions of each phase and letting the system adjust itself to steady-state conditions, the relative permeability relations were determined from the knowledge of the flowing fractions and the measured pressures and temperatures. To determine the flowing fractions it was necessary that the enthalpy of the injected fluid be known accurately. Thus it was important that the injected fractions of the components in the core be known before injection and the phase change accompanying pressure drop be considered.

After mounting the apparatus in X-ray CT equipment, the experiment was initiated by first determining the porosity of the core. This was done by taking X-ray CT scans of the core at various locations when it was dry and again when it was fully saturated with water. First, the core was kept under vacuum for several hours and the initial scan, referred to as the ***dry scan***, was performed to obtain $CT_{dry}$ values. Following this, a steady stream of water at low flow rate (5 cc/min) for sufficiently long time (12 hours) to saturate the core completely with water. A second scan, referred to as the ***wet scan***, was then conducted to obtain $CT_{wet}$ values at the same locations as the ***dry scan*** was performed. By using Equation 1 and these two sets of images obtained at every paint scanned it was possible to determine the porosity distribution of the core. Figure 2 shows porosity images obtained at four locations along the core although we obtained a total of 42 such slices during the experiment. Average porosity profiles were also calculated by averaging porosities over each slice along the core and these are shown in Figure **3.** Average porosity of the core was found to be about 22%. After the porosity distribution

had been determined the absolute permeability was determined by flowing water at different flow rates and measuring pressures along the core. From this test, the permeability of the core was calculated to be 1200 md.

Steady-state conditions were identified by the stabilization of temperature and pressure. Typically stabilization took three to five hours, though some of the measurements reported here were taken after at least six hours. Once a steady state had been confirmed, the measurements of temperature and pressure were recorded together with the heat flux sensors readings. The X-ray CT scans were then taken at locations where the dry and wet scans had been taken to obtain $CT_{exp}$ values. These scans were then processed into saturation images using Equations 2 and 3. The saturation profiles presented in this paper were obtained by averaging the saturation values over a cross sectional area of the core.

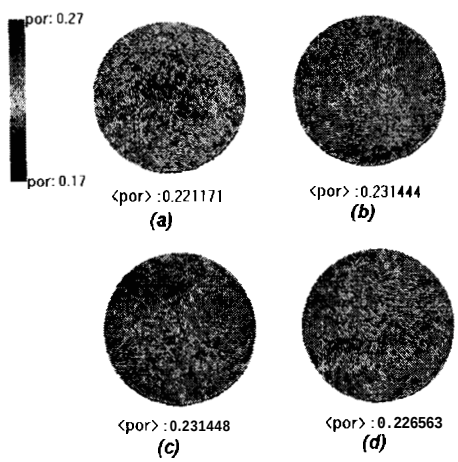


Figure 2: Selected images for porosity distributions obtained from the X-ray CT scan at 1, 11, 21 and 40 cm away from the inlet of the core.

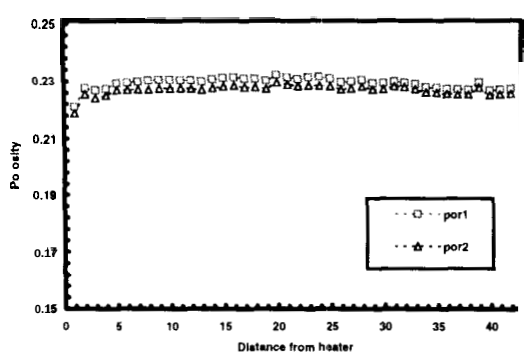


Figure 3: Average porosity profiles obtained during the experiment.

To determine whether the steam saturation distributions were in fact uniform each image had to be examined. In general, all of the images showed very uniform saturations for most sections for all flow rates, except closer to the inlet end of the core. Figure 4 shows steam saturation distributions at four locations along the core. As shown in the first image of the figure, more water exists at the top while more steam is at the bottom of the cross-sectional area at 1 cm (Figure 4a). These situation existed simply because we injected the superheated steam from the bottom portion of the end plate while the hot water from the top portion. The two phases (superheated steam and subcooled water) were mixed somewhere inside porous medium. The examination of all of the 42 slices revealed that steam and hot water were mixed at three cm from the inlet, resulting in saturated conditions. This is also apparent from the following three slices given in Figure 4b, c and d.

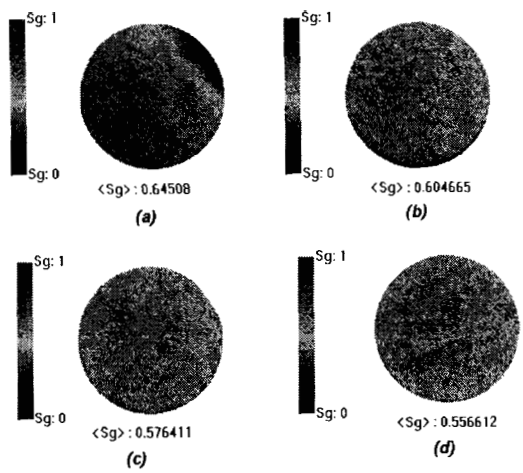


Figure 4: Selected images for steam saturation distributions obtained from the X-ray CT scan at 1, 11, 21 and 40 cm away from the inlet of the core.

During the experiment, the phase fractions of the injected fluids were changed 20 times while attempting to change the steam fraction (and steam saturation in the core). Each of these 20 steps will be referred as steps in this description. Figure 5 shows all of the average saturation profiles obtained during the experiments. In general all of the saturation profiles show a decreasing trend from the injection end to the production end. This was also observed in the numerical simulation results for the non-adiabatic case (see Satik et al., 1995). As seen from all of the steps given in the Figure, the values of steam saturation are not constant but change slightly. However, these saturation values change very little over the most of the core length and can be represented by an average value over an interval. The saturation profiles shown in Figure 5 reveal another

interesting feature. The capillary end-effects are observed at low steam flow rates with high steam fraction (e.g. Steps 10 and 11).

Table 1: Summary of the steps used during the experiment.

| Step | $q_{water}$, cc/min | $q_{steam}$, cc/min | Time elapsed,min |
|---|---|---|---|
| 1 | 4.5 | 0.5 | 375 |
| 1a | 4.5 | 0.5 | 484 |
| 1b | 4.5 | 0.5 | |
| 2 | 4.5 | 0.4 | 1283 |
| 2a | 4.5 | 0.4 | |
| 3 | 4.5 | 1.0 | 1846 |
| 4 | 4.5 | 2.0 | 2047 |
| 5 | 4.5 | 2.5 | 2220 |
| 6 | 4.5 | 3.0 | 2670 |
| 7 | 4.5 | 0.8 | 2940 |
| 8 | 6.0 | 0.8 | 3035 |
| 9 | 7.5 | 0.8 | 3487 |
| 10 | 4.5 | 0.4 | 3785 |
| 11 | 4.5 | 0.3 | 3968 |
| 12 | 1.5 | 1.5 | 4217 |
| 13 | 4.0 | 0.3 | 4795 |
| 14a | 4.0 | 0.35 | 5310 |
| 14b | 4.0 | 0.35 | 5581 |
| 15 | 1.0 | 4.0 | 5733 |
| 16 | 1.0 | 1.0 | 6780 |

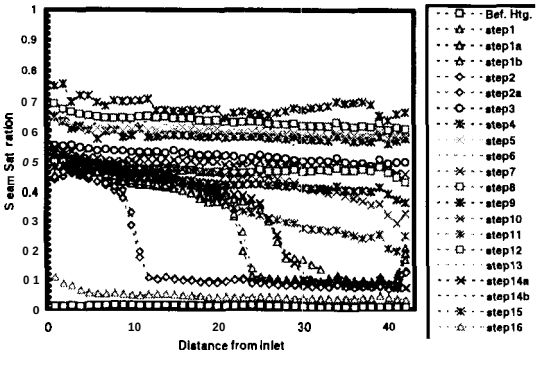


Figure 5: Average steam saturation profiles for all of the steps conducted during the experiment.

Figures 6 and 7 show steady-state temperature and pressure profiles, respectively. **As** described in the experimental apparatus section, the thermocouples were inserted through fittings for pressure taps. Thus the thermocouples made direct contact with the core sample. This was done in order to obtain the temperature measurements at the core face where the pressure readings were taken. The pressures were measured by using teflon tubes attached to the core holder body. To ensure that the readings were for the water phase these tubes were filled completely with water **up** to the transducers. By this method water in the tubes was assumed to be in contact with water in the core. In general all of the temperature and pressure measurements reflected the expected behavior i.e. decreasing values along the core from the injection end due to heat losses.

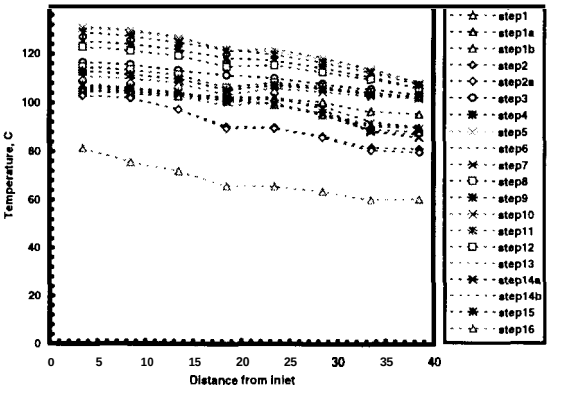


Figure 6: Temperature profiles for all of the steps conducted during the experiment.

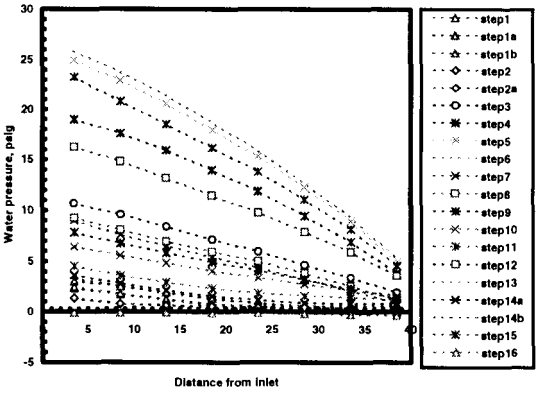


Figure 7: Pressure profiles for all of the steps conducted during the experiment.

The experiment was not conducted under perfectly adiabatic conditions because we could not use guard heaters or conduct the experiment in an oven due to limitations imposed by the X-ray CT scanner. However, an insulation material was used to minimize heat losses. Thus in the calculation of relative permeability we took heat losses into consideration and corrected the flowing phase fractions accordingly, as explained below. During the experiment, heat losses were measured only on the body of the core holder. In Figure 8, we show heat loss rate data collected during the experiment. Heat

losses were in general very similar along the core holder body and they increased as steam fraction increased.

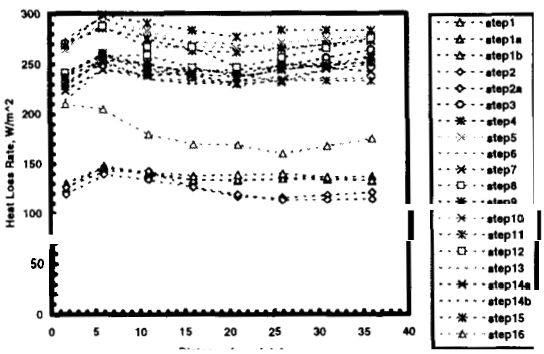


Figure 8: Heat loss rate along the core holder for all of the steps conducted during the experiment.

To calculate relative permeability we make use of the conservation equations for mass and energy fluxes:

$$m_t = m_s + m_w \quad \text{.....} \quad (4)$$

$$m_t h_t = m_s h_s + m_w h_w + Q \quad \text{.....} \quad (5)$$

where $m$ and $h$ refer to mass flow rate and enthalpy, respectively and the subscript $t$ refers to total, $s$ to vapor phase (steam) and w to the liquid phase (water), and $Q$ is the total heat lost at the point being considered. A schematic of the core holder is given in Figure 9. Using flat interface thermodynamics and mass and energy balances, the steam fraction ($X$) in the flow at any time would be given by:

$$X^1 = X^0 \frac{L_v^0}{L_v^1} + \frac{h_w^0 - h_w}{L_v^1} - \frac{QA}{m_t L_v^1} \quad \text{.....} \quad (6)$$

where $L_v$ is the latent heat of vaporization at the prevailing temperature and pressure, and A is the cross-sectional area. As demonstrated in Figure 9, superscripts 0 and 1 denote downstream and upstream of the point considered, respectively.

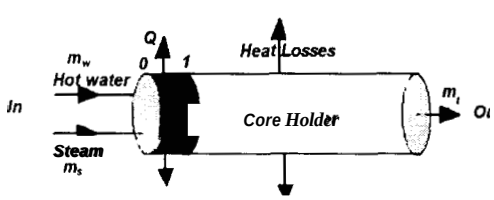


Figure 9: Schematic of the core holder for relative permeability calculations..

Then the relative permeabilities to steam and water can be calculated by using the corresponding Darcy equations for each phase in terms of the mass flow rates:

$$k_{rs} = \frac{x m_t}{\rho_s} \frac{\mu_s}{kA} \frac{\Delta p}{L} \quad \text{.....} \quad (7)$$

and

$$k_{rw} = \frac{(1-x) m_t}{\rho_w} \frac{\mu_w}{kA} \frac{\Delta p}{L} \quad \text{.....} \quad (8)$$

where $k_{rs}$, $k_{rw}$ and $k$ are steam and water relative permeabilities and absolute permeability, respectively. Thus relative permeabilities can be computed using these equations and with the knowledge of flowing mass fractions and pressure drop along a length of the core sample with a flat saturation. It is very important to know the injected enthalpy and the heat losses to evaluate the flowing fractions. Figure 8 shows the heat losses on the core body which were calculated from the measurement of the heat flux directly. In calculating the flowing fractions at a particular point, the heat loss at the point under consideration was also included.

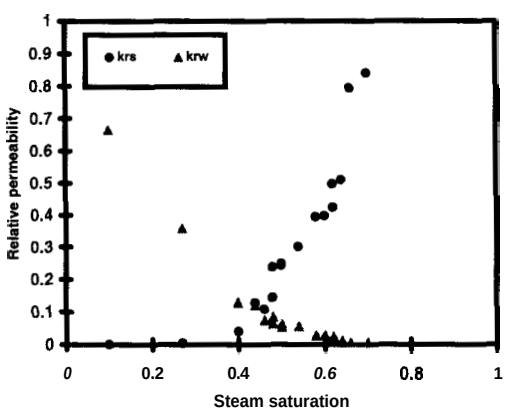


Figure 10: Relative permeability for steam and water.

In Figure 10, we show the relative permeability values calculated from the experimental data and using Equations 7 and 8 The relative permeability curves for the steam and water phases vary in a curvilinear fashion. Therefore these results do not agree with our previous results which suggested an *X-type* relationship (Ambusso, 1996). In Figure 17, we show a comparison of the steam-water relative permeability relations presented in this work to those obtained by Ambusso (1996) and Sanchez (1987). Permeability of the cores used by Ambusso (1996) and Sanchez (1987) were 600 md and 7300 md, respectively. Therefore, these results suggest a possible permeability effect on steam relative

Permeability. Further investigations to understand these differences are currently in progress. We plan to repeat the experiment with the same apparatus in order to confirm these recent results.

## CONCLUSION

In this paper, we presented a set of steam-water relative permeability curves. These results have been derived from an experiment in which the saturations within the core have been measured by using an X-ray CT scanner. A new core holder that can be used at high temperatures and pressures was designed and employed in this experiment. The core holder proved capable of withstanding the extreme conditions of the experiment A new data acquisition system was also used to collect data and to monitor the experiment.

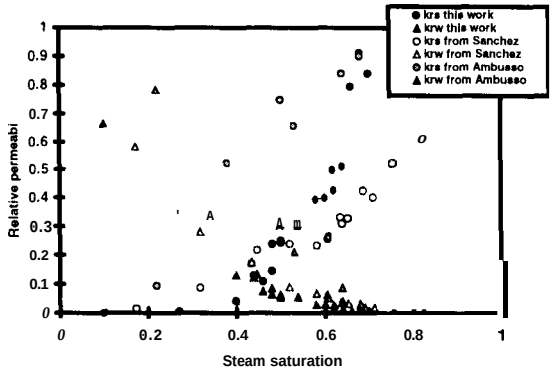


Figure 11: Comparison of steam-water relative permeability curves.

The results indicated that steam-water relative permeability vary in a curvilinear fashion with saturation as opposed to our previous results showing an "X-Type" relationship (Ambusso, 1996). However, the comparison of the results from this work to those obtained by Ambusso (1996) and Sanchez (1987) suggested a possible permeability effect on relative permeability. The residual limits for both steam and water phases were not well defined in the experiment, because it was not possible to maintain steam quality at 100% and at a very low value due to excessive condensation along the core. These end points are however inferred from the relative permeability curves and are about 30% for the water and less than 10% for the steam phase.

## ACKNOWLEDGMENTS

This work was supported by DOE contracts DE-FG07-90ID 12934 and DE-FG07-95ID 13370, the contribution of which is gratefully acknowledged. The author also would **like** to thank Roland N. Horne for his valuable comments during the course of designing the experimental apparatus, and Huda J. Nassori for the help provided during the preparation of the core holder and during assembling the experimental apparatus.

## REFERENCES

[1] W.J. Ambusso, 1996. Experimental Determination of Steam-Water Relative Permeability Relations. MS Thesis, Stanford University, Stanford. CA.

[2] W.J. Ambusso, C. Satik and R.N. Horne, 1996. **A** Study of Relative Permeability For Steam-Water Flow in Porous Media. Proc. of 21st on Stanford Workshop on Geothermal Reservoir Engineering.

[3] R.H. Brooks and A.T. Corey, 1964. Hydraulic Properties of Porous Media, Colorado State University, Hydro paper No.5.

[4] A.T. Corey, 1954. The Interrelations Between Gas and Oil Relative Permeabilities, Producers Monthly Vol. 19pp 38-41.

[5] G.L. Hassler, 1944. Method and apparatus for permeability measurements. U.S. Pat. Off., Washington, D.C., 1944.

[6] S. Ma and N. R. Morrow 1991. Effect of Firing on Petrophysical properties of Berea Sandstone, SPE Paper 21045, Presented at SPE International Symposium on Oilfield Chemistry, Anaheim, CA, Feb. 20-22.

[7] J.M. Sanchez, 1987. Surfactant Effects on the Two-Phase Flow of Steam/Water and Nitrogen/Water in an Unconsolidated Permeable Medium. Ph. D. Thesis, University of Texas, Austin, Texas.

[8] C. Satik, W. Ambusso, L.M. Castanier and. R.N. Horne, 1995. A Preliminary Study of Relative Permeability in Geothermal Rocks, GRC Trans. Vol. 19, pp 539.